

# A proton NMR study on the hydration of normal versus psoriatic stratum corneum: linking distinguishable reservoirs to anatomical structures

Cornelia Laule<sup>a,b\*</sup>, Sumia Tahir<sup>a</sup>, Charmaine L. L. Chia<sup>a</sup>, Irene M. Vavasour<sup>b</sup>, Neil Kitson<sup>c</sup> and Alex L. MacKay<sup>a,b</sup>

The NMR behaviour of normal and psoriatic stratum corneum (SC) was investigated as a function of hydration with the aim of obtaining a better understanding of the role of water in the SC structure. Time domain NMR techniques were employed to identify the signal from water and that from nonaqueous components of the SC, such as lipids and proteins. The signals were investigated as a function of water content. The free induction decay was separated into mobile signal (from water and mobile lipids) and solid signal (from protein and 'solid' lipids). Spin–spin relaxation ( $T_2$ ) measurements further separated the mobile domains within the SC. The results suggested that, when water is added to dry SC, it first enters the corneocytes; then, at a hydration of 0.24–0.33 g H<sub>2</sub>O/g SC (normal SC) or 0.12–0.24 g H<sub>2</sub>O/g SC (psoriatic SC), water begins to accumulate in hydrated lipid regions. Water was found to exchange between these two domains on the time scale of a few hundred milliseconds. When compared with normal SC, psoriatic SC had a looser corneocyte structure, a larger mobile lipid component at low hydration and a smaller capacity for corneocyte water. Copyright © 2010 John Wiley & Sons, Ltd.

**Keywords:** NMR; stratum corneum; water; psoriasis;  $T_2$  relaxation; corneocytes; mobile lipids; hydration

## INTRODUCTION

The barrier to percutaneous absorption lies within the stratum corneum (SC), the uppermost layer of the epidermis. The structure of the SC has been described as bricks and mortar (1); the corneocytes, the 'bricks', are discontinuous and embedded in a continuous intercellular domain, the 'mortar'. Consisting of insoluble bundled keratins, corneocytes are surrounded by a cell envelope which is stabilised by cross-linked proteins and covalently bound lipid. [For a review of corneocyte structure, see Elias and Feingold (2).] Polar proteinaceous structures, termed 'corneodesmosomes', interconnect the corneocytes; considerable overlap of adjacent corneocytes provides SC cohesion. The intercellular domain is highly organised, with lamellae running parallel to the skin surface. Studies have suggested that the lipids are arranged in a lamellar phase with alternating layers of water and lipid bilayers (3,4). Further complexity is introduced by the organisation of lamellar lipids into apparently 'coupled' bilayers which, unlike other lamellar structures such as myelin, have an asymmetrical distribution of interbilayer material, some of which is presumably water (5). Covalently bound lipids of the corneocyte envelope help to anchor the intercellular lipids and play an important role in SC cohesion, as well as in the permeability properties of corneocytes.

The architecture of the SC is complex, and we argue that the details of this structure determine its crucial function, namely permeability. In this sense, the SC can be modelled as a 'porous medium' (6), with the goal of such a model being to predict the permeability. Potts and Guy (7) presented a model of a 'tortuous path', with the intercellular material, particularly lipid, being the

permeability pathway through the SC, and the corneocytes being the impermeable discontinuous material. A more recent analysis (8) has suggested that corneocyte phase transport plays a significant role in SC permeability.

It is of interest that psoriatic SC, although thicker than that of uninvolved or normal skin, has increased permeability, as measured by the transepidermal water loss (9). Psoriatic corneocytes appear to be fatter and less disc-like (10) and tend to be smaller than normal corneocytes (11). The abnormalities in the morphology of psoriatic corneocytes may produce alterations in the 'porous medium' that would predict increased permeability.

\* Correspondence to: C. Laule, Department of Radiology, UBC MRI Research Centre, Room M10, Purdy Pavilion/ECU, 2221 Wesbrook Mall, Vancouver, BC, Canada, V6T 2B5.  
E-mail: claul@physics.ubc.ca

a C. Laule, S. Tahir, C. L. L. Chia, Alex L. MacKay  
Department of Physics and Astronomy, University of British Columbia, Vancouver, BC, Canada

b C. Laule, I. M. Vavasour, Alex L. MacKay  
Department of Radiology, University of British Columbia, Vancouver, BC, Canada

c N. Kitson  
Department of Medicine (Division of Dermatology), University of British Columbia, Vancouver, BC, Canada

**Abbreviations used:** CPMG, Carr–Purcell–Meiboom–Gill; DSC, differential scanning calorimetry; EPR, electron paramagnetic resonance;  $M_2$ , second moment; NNLS, non-negative least-squares; SC, stratum corneum; TR, recovery time; WC, water content.

Valuable insight has been obtained from the study of the water intake by SC as a function of relative humidity. Extracted SC lipids have been found to take on very little water until the relative humidity reaches 60–80%, with possible lipid phase transitions at higher relative humidity (12). Extracted SC corneocyte sorption data (12) have revealed gradual swelling across the whole range of relative humidity, with no evidence of phase transitions. Intact SC sorption curves (12) behave as the sum of the lipid and corneocyte curves, showing gradual swelling at lower relative humidities and accelerated swelling at higher relative humidities.

The relationship between the distribution and function of water in SC is of great interest, although not well understood (3,13–18). Water also plays a crucial role in SC physical properties, such as elasticity, and *in vitro* studies have shown that the SC is flexible as long as it contains more than 10% water (17). The inner compartment of corneocytes containing keratin is the primary location of water (2), and keratin becomes nonelastic and brittle with corneocyte water loss (4). Psoriatic skin suffers from a defective water-holding function, resulting in dry skin (9). Psoriatic SC contains lower hydration than found for normal SC at the same relative humidity and its hygroscopic properties are impaired in proportion to the severity of scaling (19). SC lipids are believed to serve a water-holding function through the formation of lamellar structures, as the removal of SC lipids by acetone/ether treatment reduces significantly the bound water content (WC) (nonfreezing water) as measured by differential scanning calorimetry (DSC) (20). Studies on extracted lipids using DSC have shown that SC lipids possess their equivalent weight in the amount of water: 0.133 mg of SC lipids can hold 0.13 mg of water in a 1 mg SC sample (20).

Most, but not all, studies have demonstrated that SC lipid structure is affected by hydration. A Fourier transform infrared spectroscopy study of human SC (21) reported only a small effect of hydration on lipid transitions over a large hydration range. X-Ray and neutron diffraction studies (22,23) revealed swelling of SC lamellae with hydration, and an electron paramagnetic resonance (EPR) spin label study (24) found that lipid transition behaviour was dependent on WC up to C12, but was independent of hydration at C16. Mobile lipid has been reported in SC preparations (25); this was modelled by a ‘sandwich’ model (4) which consists of alternating long- and short-chain ceramides and cholesterol molecules in a lamellar structure with a repeat length of 13 nm. An NMR study (12) identified a reservoir of mobile lipid in isolated porcine SC lipids. In this context, a ‘mobile’ component has an NMR signal with an exponential decay and a  $T_2$  value greater than 1 ms. The proportion of mobile lipids in isolated SC (12) increased from 24% to about 40% with increasing hydration. Similar results have been reported by Packer and Sellwood (26) in an NMR study of guinea pig SC samples hydrated by  $D_2O$ . Vavasour *et al.* (27) also found a nonaqueous fluid component of porcine SC which was assigned to lipids.

Bouwstra *et al.* (21) demonstrated, by electron micrography, that SC swelling was dominated by increases in corneocyte size and shape. They also showed that, as the WC of SC increased from a low value, corneocytes in the centre of the SC were hydrated first. At high WCs, all the corneocytes in the SC samples were swollen. This study further indicated that intercellular pockets of free water appeared in regions in which the corneocytes were maximally hydrated. Other studies have also identified these free water reservoirs (28–30).

Silva *et al.* (12) reported that hydration had a negligible effect on corneocyte mobility as measured by NMR. However, Alonso

*et al.* (31), in an EPR spin label study, showed that spin labels attached to corneocyte protein experienced increased mobility with increasing WC up to values of about 70%. This study also identified a second protein component with enhanced mobility. In an NMR study, Vavasour *et al.* (27) identified a population of nonaqueous motionally restricted protons in porcine SC, which they assigned to corneocyte protein and solid lipid. They found that the second moment, a measure of orientational order, of this population of protons decreased with increasing WC, indicating an increase in corneocyte mobility with hydration.

In the present study, we investigated the role of water in both normal human SC and SC afflicted with psoriasis. Our intent was to compare the behaviour of water in these two biological states, and to see whether any differences could lead to hypotheses concerning the role of water in permeability. Time domain NMR techniques were employed to identify the signal from water and that from nonaqueous components of the SC, such as lipids and proteins. The signals were investigated as a function of WC. The free induction decay was separated into mobile signal (from water and mobile lipids) and solid signal (from protein and ‘solid’ lipids). Spin–spin relaxation ( $T_2$ ) measurements further separated the mobile domains within the SC.

## MATERIALS AND METHODS

### Sample preparation

Normal human SC samples (BC Tissue Biobank, Vancouver, BC, Canada) were obtained by trypsinisation and stored in an airtight container until use. Psoriatic samples were removed from one location on the donor’s body by light scraping. After the removal of residual hair, the samples were cut up into small pieces and placed in a plastic weigh boat. The samples were hydrated by exposure to humidified air in a sealed chamber. Humidity was provided by an open weigh boat filled with water placed alongside the SC sample which was contained in a second weigh boat. Table 1 lists the hydrations achieved by the individual samples. As the relative humidity of the hydration chamber was less than 100%, these cannot be considered to be maximum hydrations.

After a minimum of 5 days of hydration, the SC samples were transferred into an NMR tube (outer diameter, 10 mm) and weighed. The NMR tube was capped and sealed with parafilm to prevent dehydration whilst the sample was run in the spectrometer. All samples were dehydrated incrementally with exposure to air at 50°C in the presence of the drying agent Drierite (100%  $CaSO_4$ ). The WC of the sample at each increment was defined as:

$$WC = \frac{m_{\text{sample}} - m_{\text{solid}}}{m_{\text{solid}}} \quad [1]$$

where  $m_{\text{sample}}$  is the mass of the sample at that hydration level and  $m_{\text{solid}}$  is the minimum sample weight after drying.

## NMR EQUIPMENT

$^1H$  NMR experiments were performed on a modified Bruker (Karlsruhe, Germany) SXP 4-100 NMR spectrometer operating at a frequency of 90 MHz. This spectrometer was capable of measuring the signal from all protons in the SC. The data

**Table 1.** Hydration of the normal and psoriatic stratum corneum (SC) samples

Sample	Hydration (g H <sub>2</sub> O/g SC)
Normal	
1a	0.91
1b	0.51
Psoriatic	
1	0.25
2	0.22
3a	0.54
3b	0.54
4a	0.57
4b	0.63
4c	0.80
4d	0.42
5a	0.23
5b	0.35
5c	0.44
5d	0.43

acquisition and analysis system comprised a locally built pulse programmer (32), a Rapid Systems (Seattle, Washington, USA) digitiser and an IBM-compatible computer. The digitiser dwell time was 1  $\mu$ s. All NMR experiments were carried out at an ambient temperature of 24°C.

### NMR experiments and analysis

Four NMR experiments were performed. The free induction decay and Carr–Purcell–Meiboom–Gill (CPMG) pulse sequences were performed at each hydration level, and a modified inversion recovery sequence and the cross- $T_2$  relaxation sequence were conducted at selected hydrations.

### Free induction decay

The free induction decay separated the motionally restricted (rigid or solid-like) proton signal from the signal of mobile protons, which undergo isotropic reorientation on the  $^1\text{H}$  NMR time scale of  $10^{-5}$  s. The free induction decay pulse sequence was given by  $90^\circ_x - \tau/2 - (180^\circ_y - \tau)_n$ , where  $n = 8$  and  $\tau = 400 \mu\text{s}$ . The eight  $180^\circ$  pulses were applied to refocus magnetisation dephasing caused by magnetic field inhomogeneities.

Figure 1 shows a free induction decay signal consisting of the solid and mobile components for one sample at three different hydrations. The intensities from the tops of the even echoes (representing the mobile signal) were fitted to a monoexponential function to obtain the initial mobile signal,  $M(0)$ , by extrapolation to time zero. The mobile fit was subtracted from the total signal, leaving just the motionally restricted (solid) signal. The free induction decay signal for dipolar coupled (solid) protons can be fitted to a moment expansion equation, as given by (33):

$$S(t) = S(0) \left( 1 - \frac{M_2 t^2}{2!} + \frac{M_4 t^4}{4!} + \frac{M_6 t^6}{6!} \right) \quad [2]$$

where  $M_2$ ,  $M_4$  and  $M_6$  are the second, fourth and sixth moments of the lineshape and  $S(0)$  is the total solid signal at  $t = 0$ . The signal

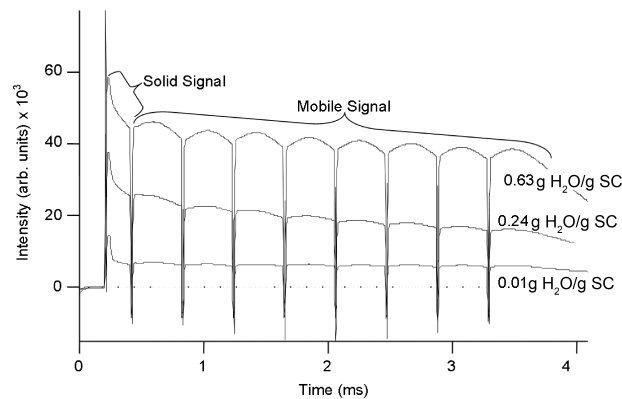


**Figure 1.**  $^1\text{H}$  NMR free induction decay of stratum corneum for three different water contents. The ratio of the mobile signal to solid signal decreases with decreasing water content, but the mobile component is not zero at approximately zero water content. The sharp dips are the  $180^\circ$  refocusing pulses, and the motionally restricted and mobile proton signals are indicated.

from the motionally restricted (solid) component was fitted to this expansion.  $M_2$  is a measure of the orientational order of proton pairs in the sample; it is large for rigid structures and decreases with the onset of molecular motions. The free induction decay also allows for the calculation of the mobile fraction ( $f_m$ ) of a sample, which is the ratio of the mobile signal (consisting of lipids and water) to the total signal, and is defined as follows:

$$f_m = \frac{M(0)}{M(0) + S(0)} \quad [3]$$

### Proton density of the solid component

To identify the solid component of the signal (assigned to rigid protein and lipid), the proton density (g H/g substance) was determined. To do this, two consecutive hydration trials ( $n$  and  $n + 1$ ) of the same sample were compared and the number of grams of hydrogen in the solid ( $\text{g H}_{\text{solid}}$ ) was calculated using:

$$\text{g H}_{\text{solid}} = \left( \frac{\Delta_{n,n+1}\text{H}_2\text{O}}{\Delta_{n,n+1}M(0)} \right) \left( \frac{2\text{gH}}{18\text{gH}_2\text{O}} \right) \overline{S(0)_{n,n+1}} \quad [4]$$

where  $\Delta_{n,n+1}\text{H}_2\text{O}$  (in grams) is the change in water mass between two trials,  $\Delta_{n,n+1}M(0)$  (in arbitrary units) is the change in mobile signal,  $2\text{gH}/18\text{gH}_2\text{O}$  is the proton density for water and  $\overline{S(0)_{n,n+1}}$  (in arbitrary units) is the average value of the solid signal.

This was repeated for several trials and an average value for  $\text{g H}_{\text{solid}}$  was obtained. To obtain a value for  $\text{g H/g solid}$ , the average  $\text{g H}_{\text{solid}}$  value was divided by the mass of the solid in the SC, assuming that 85% of the dry weight of the SC was rigid (as determined experimentally from the free induction decay at low hydration in this study).

### CPMG experiment for $T_2$ measurement

The mobile signal was further characterised into separate mobile pools based on  $T_2$  relaxation using a CPMG pulse sequence (34,35) as given by  $90^\circ_x - \tau/2 - (180^\circ_y - \tau)_n$ , with  $n = 4320$  and  $\tau = 100, 200$  or  $400 \mu\text{s}$ . A total of 736 echoes was collected. The

first 224 were collected at every echo and the remaining 512 were collected at every eighth echo. For psoriatic SC samples 3–5 and normal SC sample 1, CPMG experiments were also conducted at prehydration conditions, i.e. before the samples were hydrated.

The decay curves resulting from the CPMG sequence were decomposed into an arbitrary number of exponentials using a non-negative least-squares (NNLS) fitting routine (36) in which there were no *a priori* assumptions about the number of relaxation components. A total of 160  $T_2$  relaxation times varying from 0.001 to 10 s were input. NNLS analysis yielded a  $T_2$  distribution composed of delta functions. However, as the true  $T_2$  distribution in SC is more likely made up of a continuous distribution of relaxation times, smooth  $T_2$  distributions were obtained by allowing  $\chi^2$  to increase from 4% to 5% by minimising the surface roughness (the sum of squares of the amplitudes in the  $T_2$  distribution) as well as  $\chi^2$  (36). The geometric mean  $T_2$  relaxation time on a logarithmic scale was also calculated for the  $T_2$  distribution as follows:

$$T_2 = \exp \left[ \frac{\int S(T_2) \log T_2 dT_2}{\int S(T_2) dT_2} \right] \quad [5]$$

where the limits of the integral were specified to include the entire relaxation time distribution.

### Proton density of the mobile component

The mass of hydrogen nuclei in the nonaqueous mobile (mobile lipid at low hydration) component was determined using the following equation:

$$gH_{\text{mobile}} = \left( \frac{\Delta_{n,n+1} H_2O}{\Delta_{n,n+1} \text{Area}_{\text{water}}} \right) \left( \frac{2gH}{18gH_2O} \right) (\text{Area}_{n,n+1,\text{nonaqueous}}) \quad [6]$$

where  $\Delta_{n,n+1} H_2O$  is the difference (in grams) in the amount of water between the trials,  $\Delta_{n,n+1} \text{Area}_{\text{water}}$  is the difference (in arbitrary units) in area underneath the  $T_2$  peak corresponding to water,  $2gH/18gH_2O$  is the proton density for water and  $\text{Area}_{n,n+1,\text{nonaqueous}}$  is the average area underneath the  $T_2$  peak signifying the mobile lipid at low hydration. This  $T_2$  peak is further discussed later in the results section on spin-spin relaxation. To obtain the proton density of the mobile component, the average value of  $gH_{\text{mobile}}$  was divided by the mass of the mobile lipid in the sample, assumed to be 15% of the dry weight of the sample (as determined experimentally from the free induction decay at low hydration in this study).

### Modified inversion recovery for $T_1$ measurement

The modified inversion recovery sequence can be described as follows: (a)  $90^\circ - \text{TR}$ ; (b)  $180^\circ - \tau - 90^\circ - \text{TR}$ ; where the recovery time (TR) was 7 s and 30  $\tau$  values between 500  $\mu\text{s}$  and 5 s were chosen.

The magnetisation vector given by (b) was subtracted from the magnetisation vector given by (a), resulting in a positive signal that decayed to zero at long values of  $\tau$ . The intensity versus  $\tau$  curves were input into an NNLS algorithm, together with 160 possible  $T_1$  relaxation times ranging from 0.001 to 10 s, and a  $T_1$  distribution and geometric mean  $T_1$  were obtained in a similar manner as for  $T_2$ .

### Cross- $T_2$ relaxation

A cross- $T_2$  relaxation, Goldman-Shen (37) experiment, was carried out to determine which  $T_2$  peaks were associated with the solid component in the SC. The pulse sequence for the

experiment is given by  $90^\circ_x - 400 \mu\text{s} - (90^\circ_{-x}) - \tau_{\text{cr}} - \text{CPMG}$  (100  $\mu\text{s}$ ), where 15 values for the cross-relaxation delay time ( $\tau_{\text{cr}}$ ) were chosen between 500  $\mu\text{s}$  and 200 ms. A  $90^\circ_x$  pulse was applied and the solid-like signal was allowed to dephase. After the solid signal had dephased completely (400  $\mu\text{s}$ ), the  $90^\circ_{-x}$  pulse sent the magnetisation from the mobile protons back onto the z-axis, and magnetisation exchange was allowed to occur between the mobile and solid components during time  $\tau_{\text{cr}}$ . This was followed by a CPMG sequence with an echo spacing of 100  $\mu\text{s}$  and analysed in the same manner as the  $T_2$  relaxation data.

## RESULTS

### Hydration

Table 1 shows the hydration levels attained by the normal and psoriatic SC samples. The hydration levels attained by samples placed in the oven for the same duration varied from individual to individual and also from sample to sample.

### Proton densities

For normal SC samples 1a and 1b, the proton densities for the solid component of the SC were calculated to be 0.0449 g H/g solid and 0.0547 g H/g solid, respectively. For psoriatic samples 1 and 2, the average values were 0.0546 g H/g solid and 0.0563 g H/g solid, respectively. The expected value for protein in SC is 0.06 g H/g solid, as stated by Vavasour *et al.* (27).

Proton densities for the mobile lipids in SC were calculated to be 0.121 g H/g lipid and 0.27 g H/g lipid for normal samples 1a and 1b, respectively. The value for psoriatic sample 1 was 0.131 g H/g lipid. The expected proton density of the mobile lipid component is 0.13 g H/g lipid (27).

### Free induction decay

A comparison of free induction decay at three different hydrations for one sample (see Fig. 1) demonstrates how the mobile and motionally restricted proportions changed with WC. As the hydration decreased, the mobile component also decreased; however, it did not go to zero when the hydration approached zero, suggesting that, even after all the water was removed from the sample, a mobile component still remained.

The  $M_2$  value of the solid component of SC varied inversely with WC, as demonstrated in Fig. 2, suggesting that the dynamic orientational disorder of the motionally restricted components increased with increasing WC of the SC. All samples displayed similar trends such that, as the tissue became progressively wetter,  $M_2$  decreased. The  $M_2$  values of normal SC samples ranged from approximately  $5 \times 10^9$  to  $3 \times 10^9 \text{ s}^{-2}$ , whereas the  $M_2$  values of psoriatic SC samples ranged from  $4 \times 10^9$  to  $2 \times 10^9 \text{ s}^{-2}$ , with increasing WC. As shown in Fig. 2, the  $M_2$  values of the motionally restricted protons of the psoriatic samples were clearly lower than those of the normal SC samples.

Figure 3 shows a plot of the mobile fraction of psoriasis and normal samples as a function of WC. As the samples approached high WCs, their  $f_m$  values asymptotically approached 0.8. At low hydrations, a marked difference between normal SC samples and psoriatic SC samples was observed with regard to  $f_m$ . In completely dehydrated samples, the  $f_m$  value was not zero, indicating that another mobile component in addition to water

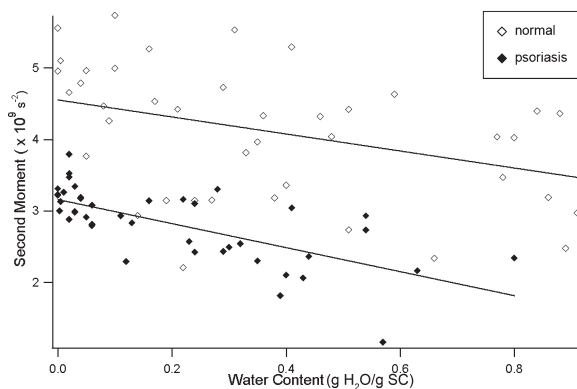


**Figure 2.** Second moment,  $M_2$ , as a function of water content for the normal (open diamonds) and psoriatic (filled diamonds) samples.  $M_2$  decreases with increasing water content, and the  $M_2$  value of psoriatic samples is lower than that of normal samples.

was present in the SC. The  $f_m$  values of both normal samples were 0.10 at zero hydration, whereas the psoriatic samples exhibited higher  $f_m$  values, ranging from 0.15 to 0.27 at zero hydration.

### Spin–spin relaxation ( $T_2$ )

The CPMG experiments were run using  $\tau$  values of 100, 200 and 400  $\mu$ s (time between 180° pulses). With the SC samples, interestingly, the three  $T_2$  distribution plots acquired at different  $\tau$  values (not shown) were different, indicating the presence of molecular motions at the 100- $\mu$ s time scale. For psoriatic samples 1 and 2, a short  $T_2$  peak (~5 ms) was present in the 100- $\mu$ s distribution but not in the 400- $\mu$ s distribution. Other differences were that the peaks were more resolved in the  $\tau = 400 \mu$ s plots and their relative intensities were not the same as in the  $\tau = 100 \mu$ s plots. However, the distributions were qualitatively similar. In this article, we focused mainly on the  $T_2$  distributions acquired at  $\tau = 400 \mu$ s.

Figures 4a and 4b show the  $T_2$  distribution plots at various WCs for normal SC sample 1a and psoriatic SC sample 4, respectively. At low hydrations, only two peaks were observed for the normal

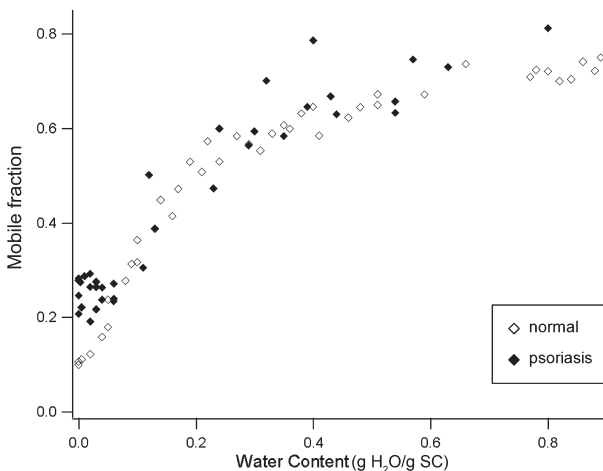


**Figure 3.** Mobile fraction signal from the free induction decay experiment as a function of water content for normal (open diamonds) and psoriatic (filled diamonds) stratum corneum samples.

sample, one with  $T_2 = 18$  ms and the other with  $T_2$  roughly between 70 and 100 ms. For the psoriatic sample, the  $T_2$  peaks at low hydration were fairly broad, with  $T_2$  values of 10 and 20 ms. On further hydration, a third peak appeared in both types of SC at a  $T_2$  value of approximately 3–5 ms. This short  $T_2$  peak increased in amplitude and shifted to longer  $T_2$  values. This shifting occurred around a WC of 0.24–0.33 g H<sub>2</sub>O/g SC for normal samples, and around 0.12–0.24 g H<sub>2</sub>O/g SC for psoriatic samples. For normal samples, the peak that was originally at 18 ms (middle  $T_2$  peak) started to increase in amplitude around 0.24 g H<sub>2</sub>O/g SC and shifted to longer  $T_2$  values on further hydration. For psoriatic samples, a middle peak (~30 ms) was observed at a hydration of 0.12 g H<sub>2</sub>O/g SC; this peak also increased in amplitude and shifted to longer  $T_2$  values. In the normal samples, the long  $T_2$  peak (around 70–100 ms) remained fairly constant in amplitude at all WCs, but shifted to longer  $T_2$  values with hydration. In the psoriatic samples, however, this long  $T_2$  peak increased in amplitude on hydration. At the maximum hydration levels reached, most of the signal was contained in the short  $T_2$  peak for normal samples, whereas, for psoriatic samples, most of the signal was contained in the middle  $T_2$  peak.

For psoriatic SC samples 3–5, CPMG experiments were conducted at prehydration conditions. The  $T_2$  distributions of all of these samples prior to hydration were quite similar, with the presence of two peaks, one around 18 ms and the other near 70 ms. Normal SC sample 1 was also run at prehydration condi-

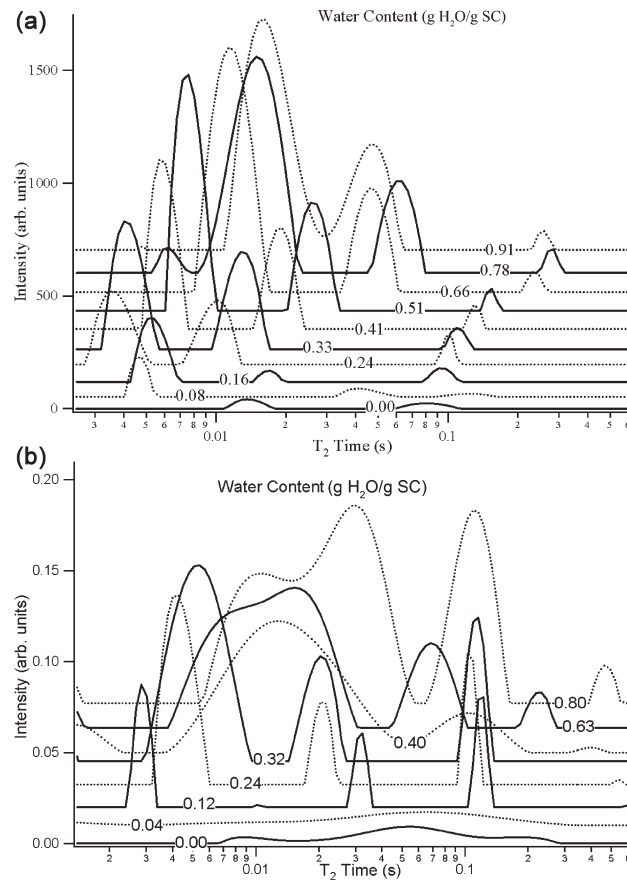


**Figure 4.** (a)  $T_2$  distribution ( $\tau = 400 \mu$ s) of normal stratum corneum (SC) sample 1a for various water contents. (b)  $T_2$  distribution ( $\tau = 400 \mu$ s) of psoriatic SC sample 4(a, b, c) for various water contents.

tions, and two peaks were observed at roughly 14 and 75 ms. Of interest are the relative proportions of the two peaks. In normal SC, the shorter  $T_2$  peak comprised about 72% of the total signal, whereas, in psoriatic SC, the shorter  $T_2$  peak comprised about 32 ± 6% of the signal.

In Fig. 5, the geometric mean  $T_2$  value is plotted as a function of WC for psoriatic and normal samples. The geometric mean  $T_2$  value decreased until a hydration of approximately 0.20 g H<sub>2</sub>O/g SC and then increased again. The psoriatic samples showed a slightly longer geometric mean  $T_2$  value at all hydrations.

### Spin-lattice relaxation ( $T_1$ )

In both the normal and psoriatic SC samples, one broad  $T_1$  peak was observed at all hydrations. A representative  $T_1$  distribution is shown in Fig. 6a. The  $T_1$  peak of normal SC samples shifted to a shorter  $T_1$  value (~140 ms) on dehydration and then started to shift back to longer  $T_1$  values around a hydration of 0.27–0.33 g H<sub>2</sub>O/g SC. The  $T_1$  distribution of psoriatic samples followed a similar trend. On hydration, the broad  $T_1$  peak first shifted to shorter  $T_1$  values and then shifted back to longer  $T_1$  values at around 0.24 g H<sub>2</sub>O/g SC for psoriatic sample 4. To characterise the  $T_1$  shift, the geometric mean  $T_1$  value was calculated, as shown in Fig. 6b. For both normal and psoriatic tissue, the geometric mean  $T_1$  value decreased up to a hydration of about 0.20 g H<sub>2</sub>O/g SC and then increased. The geometric mean  $T_1$  plots were similar in shape to the geometric mean  $T_2$  plots.

### Cross- $T_2$ relaxation

The results of the cross- $T_2$  relaxation experiment on a psoriatic sample hydrated to 0.39 g H<sub>2</sub>O/g SC are shown in Fig. 7a. The results are plotted for three  $\tau_{cr}$  values, together with the original CPMG ( $\tau = 100 \mu\text{s}$ ) distribution. All three peaks were affected by cross-relaxation; however, the short  $T_2$  peak was affected substantially more than the other peaks. This can be more clearly seen in Fig. 7b, where the intensities of the peaks (relative to the intensities of the CPMG experiment with no cross-relaxation) are plotted versus  $\tau_{cr}$ .

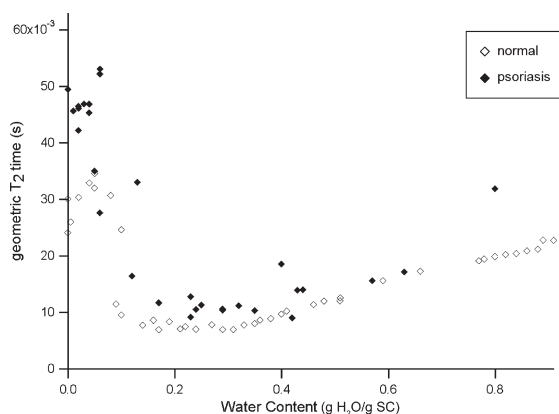


**Figure 5.** Geometric mean  $T_2$  value as a function of water content of normal (open diamonds) and psoriatic (filled diamonds) stratum corneum samples.

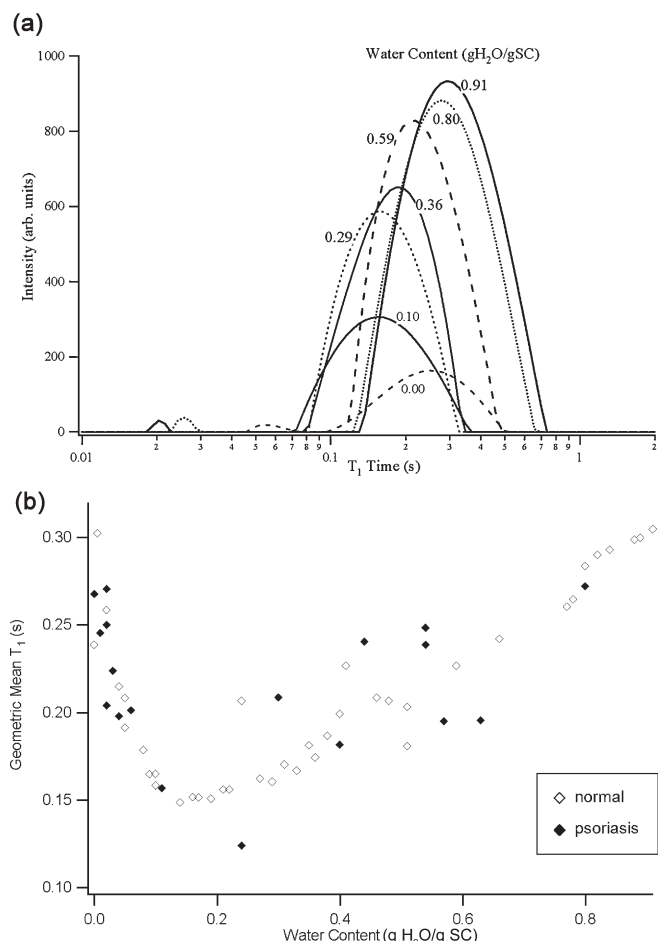


**Figure 6.** (a)  $T_1$  distribution from normal stratum corneum sample 1a for various water contents. (b) Geometric mean  $T_1$  values for various water contents for normal (open diamonds) and psoriatic (filled diamonds) samples.

## DISCUSSION

In this study, it was found that, in normal SC, as WC increased, the orientational order of the motionally restricted fraction decreased and the  $T_1$  and  $T_2$  distributions changed substantially. It was also found that psoriatic SC had a higher mobile fraction at low hydrations than did normal SC,  $M_2$  of the solid component of psoriatic SC was lower than that of normal SC at all hydrations, and the shift in the short  $T_2$  peak to longer  $T_2$  values occurred at a lower hydration in psoriatic SC.

Although the levels of hydration varied from sample to sample, except for the psoriatic mobile lipid component at low hydration, the NMR parameters for normal SC and psoriatic SC were observed to be similar for different samples at similar hydration, as illustrated by the narrow spread of the data in the curves plotted in Figs. 2, 3, 5 and 6b, which were derived from multiple samples. This similarity of the curves also suggests a negligible effect of trypsin on the normal samples, which were prepared by trypsinisation whereas the psoriatic samples were not.

### Hydration

This study supports previous observations indicating that, under identical conditions, psoriatic SC does not absorb as much water

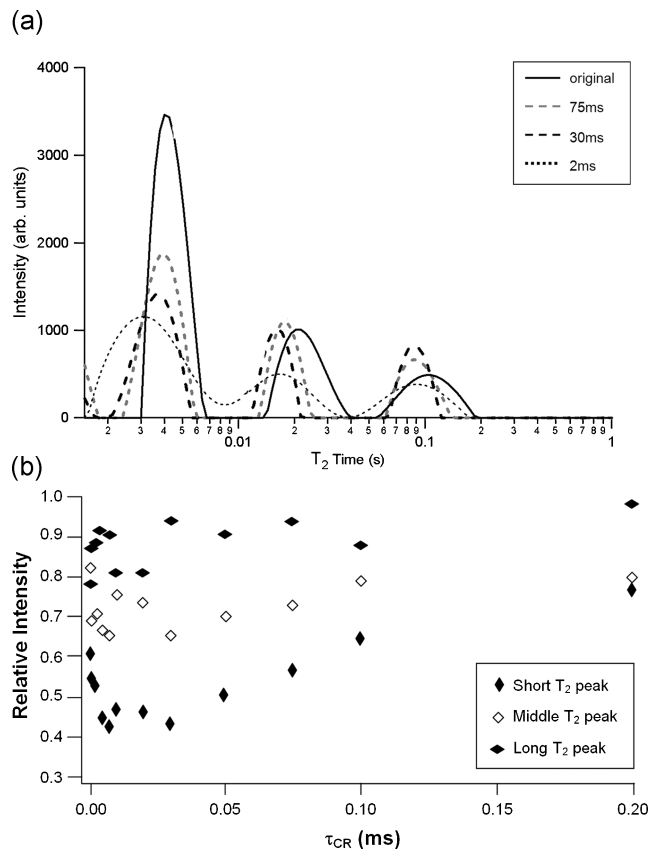


**Figure 7.** (a) Cross- $T_2$  distribution showing the original distribution, together with the distribution from three different  $t_{CR}$  values of 75, 30 and 2 ms. (b) Relative intensities of the short  $T_2$  peak ( $\blacklozenge$ ), the middle  $T_2$  peak ( $\lozenge$ ) and the long  $T_2$  peak ( $\blacklozenge$ ) plotted as a function of  $t_{CR}$ , the cross-relaxation time, compared with the peak intensities from the Carr-Purcell-Meiboom-Gill (CPMG) experiment with no cross-relaxation.

as does normal SC (13,17). Even after 9 days of hydration at a higher temperature than the normal samples, psoriatic SC did not take up as much water as normal SC hydrated for 5 days (0.80 g H<sub>2</sub>O/g SC versus 0.91 g H<sub>2</sub>O/g SC).

### Proton densities

The estimated values for the proton densities suggested that the solid signal originated largely from protein and the nonaqueous mobile component originated largely from lipid. Of course, the solid signal also contains contributions from relatively solid lipid molecules. However, we discuss later in the 'mobile fraction' section that, as the SC hydration increased, there appeared to be contributions to the mobile NMR signal from proteins. The results also indicate that the behaviour of the protein and lipid in psoriatic samples was similar to that of the same components in normal SC.

### Second moment ( $M_2$ )

The second moment ( $M_2$ ) represents the second moment of the dipolar-broadened lineshape from protons on motionally restricted sites. The measured  $M_2$  value can be decreased as a result of oscillations at the end of polymer chains or low-

amplitude rocking of molecules, i.e. anisotropic motions that are rapid on the proton NMR time scale of about 10  $\mu$ s. The  $M_2$  values of the solid component of the psoriatic samples were lower than those of the normal samples, especially at high WCs. This indicates that the solid component in psoriatic SC – keratin fibres and solid lipids – showed greater mobility than that in normal SC. This is consistent with a looser structure. Keratin and solid lipid molecules loosen on hydration; this was reflected in the decrease in  $M_2$  with increasing hydration. These results are consistent with those obtained by Vavasour *et al.* (27) in their study of porcine SC, but not with the study by Silva *et al.* (12), where it was reported that corneocyte mobility was hydration independent.

Solid proteins, e.g. rhodopsin, have  $M_2$  values of about  $5.0 \times 10^9$  s<sup>-2</sup> (38,39), and gel phase phospholipids have  $M_2$  values in the same range. Liquid crystalline phase phospholipids have  $M_2$  values an order of magnitude lower than this. The  $M_2$  values measured here for the solid SC signal are consistent with those of solid protein and gel phase hydrocarbon chains, but not with liquid crystalline hydrocarbon chains. The discrepancy between the conclusions with regard to corneocyte mobility of this study and that by Silva *et al.* (12) may simply be a consequence of the higher sensitivity of  $M_2$  to orientational order.

### Mobile fraction

The mobile signal in dry SC has been attributed previously to mobile lipids in the SC (12,26,27). At low hydrations, a marked difference between normal SC samples and psoriatic SC samples was observed with regard to  $f_m$ . Although normal samples had  $f_m = 0.10$  at low hydrations, the  $f_m$  value of psoriatic samples ranged from 0.15 to 0.27. For comparison, Vavasour *et al.* (27) found a mobile component corresponding to  $f_m = 0.13$  in dehydrated porcine SC. Up to a WC of about 0.05 g H<sub>2</sub>O/g SC, the  $f_m$  values of the psoriatic samples were fairly constant. This was also observed with porcine SC (27), but this trend was not clear with the normal SC data. As  $f_m$  is the ratio of the mobile signal to the total signal, this suggests that, compared with normal SC, psoriatic SC may have more mobile lipids or less solid tissue at low hydrations. Both interpretations are supported by the literature: one study reported an increase in mobile sterols and mobile fatty acids in psoriatic scale (9), and another showed a reduction of the characteristic high-molecular-weight keratins in psoriatic epidermis using biochemical analysis (40).

It cannot be assumed that the amount of nonaqueous SC signal which is mobile is independent of hydration; indeed, studies by Packer and Sellwood (26) and Silva *et al.* (12) have suggested that the mobile lipid fraction increases substantially as water is added to dry SC. If we normalise to the nonaqueous proton signal, we can fit eqn (3) to the curves in Fig. 3 using  $M(0) = S_{\text{mobile}}(\text{WC}) + \text{WC}$  and  $S(0) = 1 - S_{\text{mobile}}(\text{WC})$ , where  $S_{\text{mobile}}(\text{WC})$  is the relative number of nonaqueous protons which undergo fast isotropic motion and WC is the relative number of protons in water. The behaviour of  $S_{\text{mobile}}$  with hydration (see Fig. 8) is similar to that reported by Packer and Sellwood (26). For both psoriatic SC and normal SC,  $S_{\text{mobile}}$  approached 0.5 at the higher WCs, in agreement with the literature (26). The additional mobile signal at high WC could arise from lipid transitioning out of the gel state into a fluid state and/or from protein which 'loosens' at high WC. However, as concluded by Parker and Sellwood (26) and Alonso (31), it seems likely that, at the highest WCs, where  $S_{\text{mobile}}$  approaches 0.5, some protein as well as lipid contributes to the mobile signal.

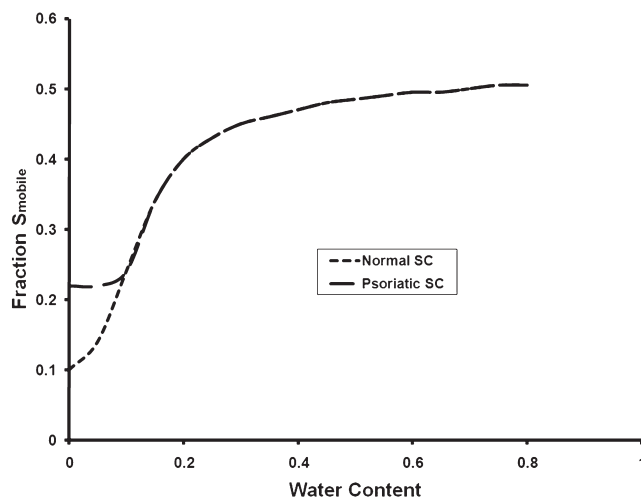


**Figure 8.** The fractional amount of isotropically narrowed nonaqueous NMR signal as a function of water content. At low hydrations, this component most probably arises from mobile lipid; however, at larger hydrations, there may be contributions to this signal from protein. SC, stratum corneum.

### Spin–spin relaxation time ( $T_2$ )

In the driest samples, we observed a small  $T_2$  peak at about 10 ms; this peak may arise from water located between the lipid bilayers.

The shortest  $T_2$  peak ( $T_2 \sim 5$  ms) increased most strongly with hydration at low WCs and was assigned to water in the corneocytes, which are the primary sites for water in the SC and also comprise the largest compartment of the SC. This assignment was supported by the cross- $T_2$  relaxation experiments, which revealed that the short  $T_2$  peak was affected most strongly by magnetisation transfer from the solid signal (which is largely from protein). The  $T_2$  value of the shortest peak increased with WC, presumably because interactions between water and the keratin chains are diminished as a result of dilution as the corneocytes swell.

We have suggested that the middle  $T_2$  peak originates from water associated with the lipid component in the SC, which is known to hydrate at higher relative humidity than does the corneocyte component (12). As the amount of water in this reservoir (hydrated lipids) increased, the  $T_2$  value of this intermediate peak increased, as would be expected for relaxation which is dominated by surface interactions. Alternatively, the middle  $T_2$  peak could have been assigned to water in intercellular pockets, where the corneocytes are maximally hydrated (21,28–30). Although intercellular pockets of water (21,28–30) might also produce a similar middle  $T_2$  peak, these pockets of water probably only arise at extremely high hydrations. Therefore, this alternative assignment seems unlikely for our SC samples, as they were well equilibrated at WCs of less than 100%.

We hypothesise that the onset of the middle  $T_2$  peak occurs when the corneocytes in a region of SC are filled and water begins to accumulate in the hydrated lipid component of the SC. For normal SC samples, the shift occurred around 0.24–0.33 g H<sub>2</sub>O/g SC, whereas, for psoriatic samples, the shift occurred at a WC of around 0.12–0.24 g H<sub>2</sub>O/g SC. This result suggests that psoriatic corneocytes take up less water than normal corneocytes, partly because psoriatic corneocytes are smaller than normal corneocytes, as mentioned previously. Furthermore, the psoriatic corne-

ocyte envelope has been found to be abnormal and lacks certain covalently bound lipids which are important for the barrier properties of the envelope. It has been reported that the total content of bound lipid is the same in both normal SC and psoriatic scale, but more fatty acids and less ceramide B are present in psoriatic scale (41). Another study reported a reduction in ceramide 1 (sphingosine) in psoriatic plaques; ceramide 1 is important for water retention (9). Covalently bound lipid may restrict the diffusion of water across the envelopes (42). As a result of such defects in the envelope of psoriatic corneocytes, the rate of diffusion across the barrier is probably increased and, consequently, water ‘leaks out’ of the psoriatic corneocytes, leading to rapid dehydration – a characteristic of psoriatic scale.

The middle  $T_2$  peak, attributed to water within the lipid region, dominated the  $T_2$  distribution at high hydrations (~0.40 g H<sub>2</sub>O/g SC) in psoriatic SC, but not in normal SC. In normal SC, the shortest  $T_2$  peak, assigned to water in the corneocytes, still contained most of the signal at the highest WCs.

The longest  $T_2$  peak was assigned to the signal from lipids because, unlike the short  $T_2$  peak, the longest  $T_2$  peak did not disappear on complete dehydration. In addition, the longest  $T_2$  peak was the least affected by magnetisation transfer from the solid signal (Fig. 7b). Furthermore, Vavasour *et al.* (27) found that protons from the longest  $T_2$  peak did not exchange with heavy water protons, and that the NMR spectrum of completely dehydrated SC showed a peak at 1.8 p.p.m. which is close to the chemical shift of CH<sub>2</sub> and CH<sub>3</sub> (protons in hydrocarbon chains).

Given the substantial increase in  $S_{\text{mobile}}$  at higher WCs, we would expect this increased mobile signal to contribute to the  $T_2$  distribution. We have assumed that this signal contributed to the long  $T_2$  peak; however, this cannot be substantiated with these data.

Differences were observed between the  $T_2$  plots acquired at  $\tau$  values of 100, 200 and 400  $\mu$ s, especially at higher hydrations. The differences indicate that molecular motions are occurring within a time scale of 100–200  $\mu$ s. As the difference between  $\tau = 100$   $\mu$ s and  $\tau = 400$   $\mu$ s was demonstrated predominantly by changes in the intensities of the shortest and middle peaks, we speculate that, at this time scale, exchange of water takes place between the corneocytes and the hydrated lipid regions. Such an exchange would affect the amplitudes and times of these two water  $T_2$  peaks.

### Spin-lattice relaxation time ( $T_1$ )

The appearance of a single peak in the  $T_1$  distribution indicates that magnetisation exchange takes place between the separate compartments within the SC (i.e. water molecules move between compartments on the  $T_1$  time scale of several hundred milliseconds). For both types of SC, the geometric mean  $T_1$  showed a minimum at a WC of about 0.20 g H<sub>2</sub>O/g SC. This trend may be explained as follows. At low hydrations, the mobile component in the SC is predominantly lipid, which has a long  $T_1$  value, and so the geometric mean  $T_1$  value is also long. On hydration of the SC, water is incorporated into the tissue (corneocytes and lipid structures) and, because of the close interaction of water with the SC, the  $T_1$  value of water is relatively short. Therefore, when the WC is comparable with the lipid content of the SC, the geometric mean  $T_1$  value is significantly affected by the shorter  $T_1$  of water, and so the geometric mean  $T_1$  value decreases. With further hydration, the additional water is not as closely associated with nonaqueous SC tissue, and hence has a longer  $T_1$  value.

### Prehydration results

It is worth noting that the  $f_m$  values of psoriatic samples in the prehydration state were the same or lower than those of dehydrated samples. This indicates that the psoriatic samples were almost completely dry when obtained from the patients, in agreement with observations that prehydration WC values for psoriatic scale are nearly always zero (19). This also indicates that the process of hydration followed by dehydration did not cause irreversible structural changes to the SC samples.

### CONCLUSIONS

This study has demonstrated that, at physiological hydrations, most water in the SC is located in the corneocytes. The orientational order of the corneocytes decreased with increasing WC. As the WC of SC increased, the corneocytes filled, and water then accumulated in hydrated lipid regions.

At very low WCs, more mobile lipid was found in psoriatic SC than in normal SC. Compared with normal SC, psoriatic SC corneocytes held less water and had a lower orientational order.

### Acknowledgements

We wish to thank Ian MacKenzie for his assistance in the preparation of the normal tissue samples and the patients who donated psoriatic tissue samples. This project was supported by the Natural Sciences and Engineering Research Council (NSERC) Discovery Grant to Alex MacKay and an NSERC Research Studentship awarded to Sumia Tahir. We are particularly appreciative of the constructive criticisms provided by the reviewers of the manuscript.

### REFERENCES

- Elias PM. Structure and function of the stratum corneum permeability barrier. *Drug Dev. Res.* 2004; 13: 97–105.
- Elias PM, Feingold KR. *Skin Barrier*. Taylor & Francis Group: New York, 2005; 612.
- Charalambopoulou GC, Steriotis TA, Stefanopoulos KL, Mitropoulos AC, Kanellopoulos NK, Keiderling U. Investigation of lipid organization on stratum corneum by water absorption in conjunction with neutron scattering. *Physica B: Phys. Condensed Matter*, 2000; 276: 530–531.
- Forslind B. A domain mosaic model of the skin barrier. *Acta Derm. Venereol.* 1994; 74: 1–6.
- McIntosh TJ. Organization of skin stratum corneum extracellular lamellae: diffraction evidence for asymmetric distribution of cholesterol. *Bioophys. J.* 2003; 85: 1675–1681.
- Kitson N, Thewalt JL. Hypothesis: the epidermal permeability barrier is a porous medium. *Acta Derm. Venereol. Suppl. (Stockh.)* 2000; 208: 12–15.
- Potts RO, Guy RH. Predicting skin permeability. *Pharm. Res.* 1992; 9: 663–669.
- Wang TF, Kasting GB, Nitsche JM. A multiphase microscopic diffusion model for stratum corneum permeability. I. Formulation, solution, and illustrative results for representative compounds. *J. Pharm. Sci.* 2006; 95: 620–648.
- Motta S, Monti M, Sesana S, Mellesi L, Ghidoni R, Caputo R. Abnormality of water barrier function in psoriasis. Role of ceramide fractions. *Arch. Dermatol.* 1994; 130: 452–456.
- Marks R, Barton S. The significance of the size and shape of corneocytes. *Proceedings of the International Symposium on the Stratum Corneum, Cardiff*, Springer-Verlag: Berlin; 161.
- Grove G, Kligman A. Corneocyte size as an indirect measure of epidermal proliferative activity. *Proceedings of the International Symposium on the Stratum Corneum, Cardiff*, Springer-Verlag: Berlin; 191.
- Silva CL, Topgaard D, Kocherbitov V, Sousa JJ, Pais AA, Sparr E. Stratum corneum hydration: phase transformations and mobility in stratum corneum, extracted lipids and isolated corneocytes. *Biochim. Biophys. Acta*, 2007; 1768: 2647–2659.
- Borroni G, Vignati G, Brazzelli V, Vignoli GP, Gabba P, Gatti M, Berardesca E, Cossetta A, Rabbiosi G. Changes in the water holding capacity of psoriatic stratum corneum in vivo. *Acta Derm. Venereol. Suppl. (Stockh.)* 1989; 146: 192–194.
- Bouwstra J, Gooris G, Salomons-de Vries M, van der Spek J, Bras W. Structure of human stratum corneum as a function of temperature and hydration: a wide-angle X-ray diffraction study. *Int. J. Pharm.* 1992; 84: 205–261.
- Edwards PA, Walker M, Gardner RS, Jacques E. The use of FT-IR for the determination of stratum corneum hydration in vitro and in vivo. *J. Pharm. Biomed. Anal.* 1991; 9: 1089–1094.
- Menon GK, Elias PM. Morphologic basis for a pore-pathway in mammalian stratum corneum. *Skin Pharmacol.* 1997; 10: 235–246.
- Takenouchi M, Suzuki H, Tagami H. Hydration characteristics of pathologic stratum corneum – evaluation of bound water. *J. Invest. Dermatol.* 1986; 87: 574–576.
- Warner RR, Boissy YL, Lilly NA, Spears MJ, McKillop K, Marshall JL, Stone KJ. Water disrupts stratum corneum lipid lamellae: damage is similar to surfactants. *J. Invest. Dermatol.* 1999; 113: 960–966.
- Tagami H, Iwase Y, Yoshikuni K, Inoue K, Yamada M. Water sorption-desorption test of the stratum corneum of the skin surface in vivo. *Proceedings of the International Symposium on the Stratum Corneum, Cardiff*, Springer-Verlag: Berlin; 248.
- Imokawa G, Kuno H, Kawai M. Stratum corneum lipids serve as a bound-water modulator. *J. Invest. Dermatol.* 1991; 96: 845–851.
- Bouwstra JA, de Graaff A, Gooris GS, Nijssse J, Wiechers JW, van Aelst AC. Water distribution and related morphology in human stratum corneum at different hydration levels. *J. Invest. Dermatol.* 2003; 120: 750–758.
- Ohta N, Ban S, Tanaka H, Nakata S, Hatta I. Swelling of intercellular lipid lamellar structure with short repeat distance in hairless mouse stratum corneum as studied by X-ray diffraction. *Chem. Phys. Lipids.* 2003; 123: 1–8.
- Charalambopoulou G, Steriotis T, Hauss T, Stubos A, Kanellopoulos N. Structural alterations of fully hydrated human stratum corneum. *Phys. Rev. B Condens. Matter.* 2004; 350 (Suppl 1): E603–E606.
- Alonso A, Meirelles NC, Tabak M. Effect of hydration upon the fluidity of intercellular membranes of stratum corneum: an EPR study. *Biochim. Biophys. Acta*, 1995; 1237: 6–15.
- Bouwstra JA, Gooris GS, Dubbelaar FE, Ponec M. Phase behavior of lipid mixtures based on human ceramides: coexistence of crystalline and liquid phases. *J. Lipid Res.* 2001; 42: 1759–1770.
- Packer K, Sellwood T. Proton magnetic resonance studies of hydrated stratum corneum. Part 1. Spin-lattice and transverse relaxation. *J. Chem. Soc., Faraday Trans. 2*, 1978; 74: 1579–1591.
- Vavasour I, Kitson N, MacKay A. What's water got to do with it? A nuclear magnetic resonance study of molecular motion in pig stratum corneum. *J. Invest. Dermatol. Symp. Proc.* 1998; 3: 101–104.
- Warner RR, Stone KJ, Boissy YL. Hydration disrupts human stratum corneum ultrastructure. *J. Invest. Dermatol.* 2003; 120: 275–284.
- Bouwstra JA, Honeywell-Nguyen PL, Gooris GS, Ponec M. Structure of the skin barrier and its modulation by vesicular formulations. *Prog. Lipid Res.* 2003; 42: 1–36.
- Pieper J, Charalambopoulou GC, Steriotis TA, Vasenkov S, Desmedt A, Lechner R. Water diffusion in fully hydrated porcine stratum corneum. *Chem. Phys.* 2003; 292: 465–476.
- Alonso A, Vasques da Silva J, Tabak M. Hydration effects on the protein dynamics in stratum corneum as evaluated by EPR spectroscopy. *Biochim. Biophys. Acta*, 2003; 1646: 32–41.
- Sternin E. Data acquisition and processing: a systems approach. *Rev. Sci. Instrum.* 1985; 56: 2043–2049.
- Abraham A. *The Principles of Nuclear Magnetism*. Oxford University Press: London, 1961.
- Carr HY, Purcell EM. Effects of diffusion on free precession in nuclear magnetic resonance experiments. *Phys. Rev.* 1954; 94: 630–639.

35. Meiboom G, Gill D. Modified spin echo method for measuring relaxation times. *Rev. Sci. Instrum.* 1958; 29: 688–691.
36. Whittall KP, MacKay AL. Quantitative interpretation of NMR relaxation data. *J. Magn. Reson.* 1989; 84: 134–152.
37. Goldman M, Shen L. Spin–spin relaxation in LaF<sub>3</sub>. *Phys. Rev.* 1966; 144: 321–331.
38. MacKay AL, Burnell EE, Bienvenue A, Devaux P, Bloom M. Flexibility of membrane proteins by broad-line proton magnetic resonance. *Biochim. Biophys. Acta – Biomembranes*, 1983; 728: 460–462.
39. MacKay AL. A proton NMR moment study of the gel and liquid-crystalline phases of dipalmitoyl phosphatidylcholine. *Biophys. J.* 1981; 35: 301–313.
40. Jahn H, Nielsen EH, Elberg JJ, Bierring F, Ronne M, Brandrup F. Ultrastructure of psoriatic epidermis. *Apmis*, 1988; 96: 723–731.
41. Wertz PW, Madison KC, Downing DT. Covalently bound lipids of human stratum corneum. *J. Invest. Dermatol.* 1989; 92: 109–111.
42. Redelmeier T, Schaefer H. *Skin Barrier – Principles of Percutaneous Absorption*. Karger AG: Basle, 1996; 310.